

REVIEW SUMMARY

METAMATERIALS

Spatiotemporal light control with active metasurfaces

Amr M. Shaltout, Vladimir M. Shalaev, Mark L. Brongersma*

BACKGROUND: Metasurfaces have opened up a number of remarkable new approaches to manipulate light. These flat optical elements are constructed from a dense array of strongly scattering metallic or semiconductor nanostructures that can impart local changes to the amplitude, phase, and polarization state of light waves. They have facilitated a relaxation of the fundamental Snell's law for light refraction and enabled the creation of small form factor optical systems capable of performing many tasks that currently can only be achieved with bulky optical components. New photon management capabilities have also emerged, including the achievement of multiple optical functions within a single metasurface element, the realization of very high-numerical apertures, and dispersion engineering with metasurface building blocks. Despite this impressive progress, most metasurfaces we see today are static in nature, and their optical properties are set in stone during their fabrication. However, we are currently witnessing an evolution from passive metasurfaces to active metasurface devices. This natural progression stems from the notion that space and time play complementary roles in Maxwell's equations. It suggests that structuring materials in both space and time can bring forth new physical phenomena and fur-

ther broaden the range of possible applications. This Review discusses what is required to create high-performance spatiotemporal metasurfaces and analyzes what new applications and physics they have to offer.

ADVANCES: To realize the dream of dynamically controlled metasurfaces, we need to achieve strong and tunable light-matter interactions in ultrathin layers of material. In doing so, we cannot rely on the long interactions of lengths and times provided by bulk optical crystals or waveguides. This has stimulated much research aimed at identifying new materials and nanostructures capable of providing dramatically enhanced light-matter interaction and highly tunable optical responses. There are already well-established ways to boost light-matter interaction through the engineering of plasmonic and Mie-style resonances in metallic and semiconductor nanostructures. However, the best approaches to dynamically alter their optical response are the topic of current study.

We highlight different approaches that involve electrical gating, optical pumping, mechanical actuation, stimulating phase transitions, magneto-optical effects, electrochemical metallization, liquid-crystal control, and nanostructured nonlinearities. We also discuss how

metasurfaces can be used to realize reconfigurable devices, such as tunable lenses and holograms, optical phase modulators, and polarization converters. In addition to these emerging applications, it has become apparent that temporal control of metasurfaces at an ultrafast speed can unlock entirely new

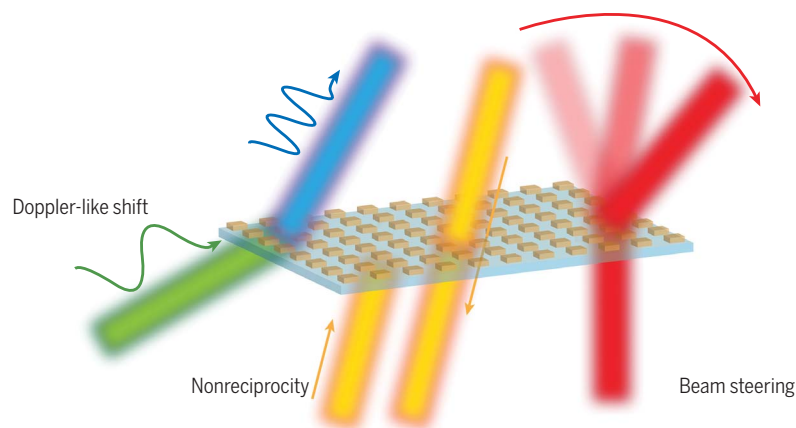
ON OUR WEBSITE

Read the full article at <http://dx.doi.org/10.1126/science.aat3100>

physical effects that are not accessible in their static counterparts. Photons interacting with spatiotemporally modulated metasurfaces can display changes in their frequency as well as their linear momentum, angular momentum, and spin. This opens the door to new operating regimes for metasurfaces in which light can experience Doppler shifts, break Lorentz reciprocity, or produce time-reversed optical beams.

OUTLOOK: The emergence of active metasurfaces is very timely given the many applications that would benefit from having tunable optical components that are flat and easy to integrate. These include a variety of wearables, autonomous vehicles, robotics, augmented and virtual reality, sensing, imaging, and display technologies. However, a massive challenge lies ahead toward realizing the full technological potential of these new elements. The ultimate unit cell of an active metasurface should be subwavelength in size and facilitate large, dynamic amplitude and phase tuning. For larger metasurfaces, the need to individually address and activate the massive number of tiny unit cells will also pose integration and power-consumption challenges that rival those that are currently faced by the semiconductor industry in the creation of the next generation of integrated circuits. If realized, such elements may radically outperform conventional systems that are based on bulky optical and mechanical parts.

As new physical effects appear in spatiotemporal metasurfaces, new fundamental questions are also bound to arise. It is already clear that the very basic processes of light absorption, modulation, fluorescent and thermal emission, frequency conversion, and polarization conversion can be manipulated in new ways. As a result, the typically assumed limits for time-invariant or reciprocal systems will need to be reconsidered in these dynamic systems. A concerted, highly interdisciplinary effort is thus required to uncover and push the bounds by which these sheets of spatiotemporally structured materials can manipulate light. ■



Optical phenomena that can be realized with spatiotemporal metasurfaces. Wavelength conversion emulating a Doppler shift, nonreciprocal transmission, and active steering of optical beams.

The list of author affiliations is available in the full article online.

*Corresponding author. Email: brongersma@stanford.edu
Cite this article as A. M. Shaltout et al., *Science* **364**, eaat3100 (2019). DOI: 10.1126/science.aat3100

REVIEW

METAMATERIALS

Spatiotemporal light control with active metasurfaces

Amr M. Shaltout¹, Vladimir M. Shalaev², Mark L. Brongersma^{1*}

Optical metasurfaces have provided us with extraordinary ways to control light by spatially structuring materials. The space-time duality in Maxwell's equations suggests that additional structuring of metasurfaces in the time domain can even further expand their impact on the field of optics. Advances toward this goal critically rely on the development of new materials and nanostructures that exhibit very large and fast changes in their optical properties in response to external stimuli. New physics is also emerging as ultrafast tuning of metasurfaces is becoming possible, including wavelength shifts that emulate the Doppler effect, Lorentz nonreciprocity, time-reversed optical behavior, and negative refraction. The large-scale manufacturing of dynamic flat optics has the potential to revolutionize many emerging technologies that require active wavefront shaping with lightweight, compact, and power-efficient components.

The metamaterials field has radically changed the way we engineer light-matter interactions and taught us how to spatially structure materials at a subwavelength scale to unlock new optical phenomena (1, 2). With the advent of mass-producible two-dimensional (2D) metamaterials, now commonly referred to as metasurfaces, the promise of metamaterials is becoming a practical reality (3–5). A myriad of passive metasurfaces have already been demonstrated and have illustrated the many ways to impart spatially varying amplitude, phase, and polarization changes on an optical wavefront. Topological and inverse design (6) concepts also have proven their value in the performance optimization of metasurfaces because they afford new ways to perfect the design and spatial arrangement of the constituent optical antennas. These advances have led to a relaxation of the fundamental Snell's law for light refraction (4) and facilitated the creation of entirely new, ultrathin, flat optical components capable of manipulating the momentum, orbital angular momentum, and spin state of photons. Despite these impressive advances, current metasurfaces are mostly static in nature, and their optical properties are set in stone during their fabrication process. Opportunities to actively control light stem from the observation that space and time play similar roles in Maxwell's equations; this suggests that further structuring of metasurfaces in the time domain can provide new opportunities to manipulate light and facilitate a transition to dynamic, flat optical devices. The first wave of active metasurfaces very

much resembles static metasurfaces in which the passive materials and building blocks (meta-atoms) are replaced by active counterparts whose optical response can be altered with an external stimulus (7). However, it is now also becoming apparent that dynamic manipulation of light waves with ultrahigh spatial and ultrafast temporal control can lead to entirely new physics. It is thus of great value to expand the family of space-variant 2D metasurfaces to (2+1)D spatiotemporally controlled metasurfaces that are structured in space and time. This Review analyzes the state of the field and arising opportunities for this new class of optical devices.

A formidable experimental challenge lies ahead in realizing the true potential of time-varying metasurfaces. Although subwavelength spatial structuring of materials can now be accomplished with a range of nanofabrication approaches, it's not trivial to implement effective temporal manipulation to render metasurfaces dynamic because these flat components can only provide very short interaction lengths and times. For this reason, most ultrafast temporal control experiments currently rely on large bulk crystals or optical waveguides that provide long interaction lengths. This has prompted a search for new materials, structures, and strategies that afford dynamic and highly tunable materials responses. One approach to boost light-matter interaction is to capitalize on optical resonances that are intrinsic to the materials used [such as excitonic and ϵ -near-zero (ENZ) resonances] or are supported by nanostructures (plasmonic or Mie resonances). Another pathway is to operate near phase transitions or critical points at which the optical materials' properties display unusually strong dependences on external control parameters, such as the carrier density, electric or magnetic field, chemical reactions, mechanical motion, or temperature. A conceptual schematic of dif-

ferent emerging metasurface modulation approaches is demonstrated in Fig. 1.

The emergence of reconfigurable metasurfaces is timely given a strong demand for cost-efficient, integrated, lightweight hardware to achieve critical optical functions for optical/quantum communication and computation, light detection and ranging (LIDAR) for autonomous vehicles, or other computational imaging applications (8–12) such as augmented reality (12), display (13), interferometry (14), and holography (13, 15). By avoiding interconversion from optical to electrical and back, spatiotemporal metasurfaces afford free-space optical modulation, and beam shaping in a more power-efficient fashion than conventional approaches. In this vein, different metasurfaces are now implemented to achieve all kinds of spatial light modulation functions, including phase modulation, polarization conversion (16), adaptive optical components (17–20), tuning spectral response (21, 22), and thermal emission control (23).

The fusing of the metasurface and ultrafast/coherent optics fields is bound to also give rise to radically new devices that are not simply active upgrades of already demonstrated passive metasurfaces. Previously inaccessible physical phenomena are also observed upon ultrafast modulation through optical pumping; the harnessing of photo-carrier excitation or ultrafast optical nonlinearities can lead to a new genus of optical devices that can overcome fundamental limitations of merely space-variant metasurfaces (24–27) to break Lorentz reciprocity (24–26) or to achieve Doppler-like wavelength shift (24, 27). This opens the door to entirely new devices that offer optical isolation without the presence of magnetic fields and new ways to realize topological protected systems (28).

Materials, building blocks, and mechanisms empowering active metasurfaces

Spatiotemporal metasurfaces can be classified based on the operational physical mechanism to achieve tuning. Mechanisms that afford sufficiently strong tuning of optical properties for their practical use in spatiotemporal metasurfaces are illustrated in Fig. 1.

Electrical gating and photocarrier excitation

One of the most common approaches to tune optical properties is through modulation of the free carrier density in conductive materials by means of electrical gating and photocarrier excitation. Transparent conducting oxides and nitrides (8–10, 29, 30) and atomically thin 2D materials (8, 14, 31, 32) display lower free-carrier densities than those of noble metals. This facilitates more effective field penetration and modulation of the permittivity by using both electrical (8–10) and optical (29, 30, 33, 34) stimuli. The achievable changes can be further enhanced by operating at the ENZ point at which the permittivity approaches zero. For example, it has been shown how permittivity changes on the order of unity can be achieved through electrical

¹Geballe Lab for Advanced Materials, Stanford University, Stanford, CA 94305, USA. ²Department of Electrical and Computer Engineering and Birck Nanotechnology Center, Purdue University, West Lafayette, IN 47906, USA.

*Corresponding author. Email: brongersma@stanford.edu

gating of indium-tin-oxide (ITO) (35). Subsequently, voltage-controlled metasurfaces using ITO have been created, and the ENZ effect has been used for low-voltage absorption modulation and steering (Fig. 2A) (9, 36).

One major obstacle toward application of this phenomenon is that the charge density and optical changes only take place in nanometer-thin accumulation or depletion layers. Gap plasmon resonators have provided a way out by offering very high field confinement and excellent mode overlap with the active switching medium. To further overcome this obstacle, dual-gated unit cells (37) have been used, in which two independent voltage-controlled channels are connected in series to achieve increased reflection phase tunability ($>300^\circ$). On the other hand, photo-carrier excitation in ITO (29, 38) and aluminum-doped zinc oxide (AZO) is also possible and offers ultrafast modulation speeds and an ability to alter properties throughout the entire materials volume (29, 30, 33, 34). The refractive index of an ITO film has demonstrated optical modulation by 170%, with a recovery time of ~ 360 fs (29). Such index tuning can also be used to notably change the spectral scattering properties of plasmonic antennas patterned on top of an ITO layer (33). Both interband and intraband optical excitations in transparent oxides have been experimentally verified and used to modulate the optical properties of these materials (30). The associated nonlinearities provide independent and opposite changes to the dielectric permittivity, adding an extra degree of freedom to control the temporal dependence of the permittivity. How interband and intraband excitations of an AZO layer can affect the transmission of light is illustrated in Fig. 2B (30).

In addition, beam shaping with lasers can be used to create desired index variations along the material surface by creating a gradient in the pump intensity across the structure. Conventional semiconductors—such as silicon, germanium, and gallium arsenide (GaAs)—do not possess free-carrier densities as high as the transparent conducting oxides, but these materials can still provide noticeable changes in optical properties in the terahertz regime. For example, a plasmonic metasurface integrated with photoconductive silicon has been implemented and successfully achieved electromagnetically induced transparency by means of optical pumping (39); the modulation is attributed to a change in the damping rate of a dark mode caused by the increased conductivity of silicon islands under photoexcitation.

Whereas applied electric fields are screened from the interior of nanoscale metallic and highly doped semiconductor systems, the charge carriers and excitons in atomically thin materials are effectively tuned with gating. Gating graphene can lead to strong absorption modulation that can be boosted by carving the material into 2D plasmonic resonators (40). Because absorption is fundamentally related to thermal emission, electronic control of blackbody emission from graphene plasmonic resonators could be demonstrated (41). Semiconductor 2D materials also exhibit large, tunable optical changes near their excitonic resonances (42). However, atomically thin layers usually require additional nanostructures or microcavities to further enhance the optical response and render them useful in metasurfaces. For example, graphene combined with metallic ring apertures (Fig. 2C) have been used to achieve 50% modulation of the trans-

mitted light intensity (32). Graphene has also been combined with plasmonic metasurfaces to achieve effective amplitude and phase modulation in the near-infrared (NIR) and mid-IR spectral ranges by either shifting or damping plasmonic resonances (31, 43–45). Optical pumping of 2D materials has also been used. Ultrafast dynamics of excited carriers in black phosphorous across visible and mid-IR wavelengths with picosecond-scale recombination times have been demonstrated (46). Optical modulation has also been applied to multilayered 2D materials, in which the interlayer van der Waals interaction in transition-metal dichalcogenides has been modulated to tune their optical properties (47). Free carrier modulation has also been achieved in quantum well materials. For example, absorption modulation of 30% has been realized by using a polaritonic coupling of plasmonic resonant modes and voltage-tunable intersubband transitions in the wells (22).

Phase-change materials

Phase-change materials such as germanium-antimony-tellurium (GST) (12, 13, 39, 48, 49), vanadium dioxide (VO_2) (20, 49–54), and gallium (Ga) (55) have featured prominently in the evolution of nanophotonic active metasurfaces. The primary reason being that structural and electronic phase transitions in these materials can result in unity-scale index changes. A particularly large contrast in the optical properties can be observed when GST is switched between amorphous and crystalline phases by using heating, electrical, or optical stimuli. This is well known from its use as a storage medium in the digital versatile disc (DVD) (56, 57) and more recently in programmable metasurfaces. Optical

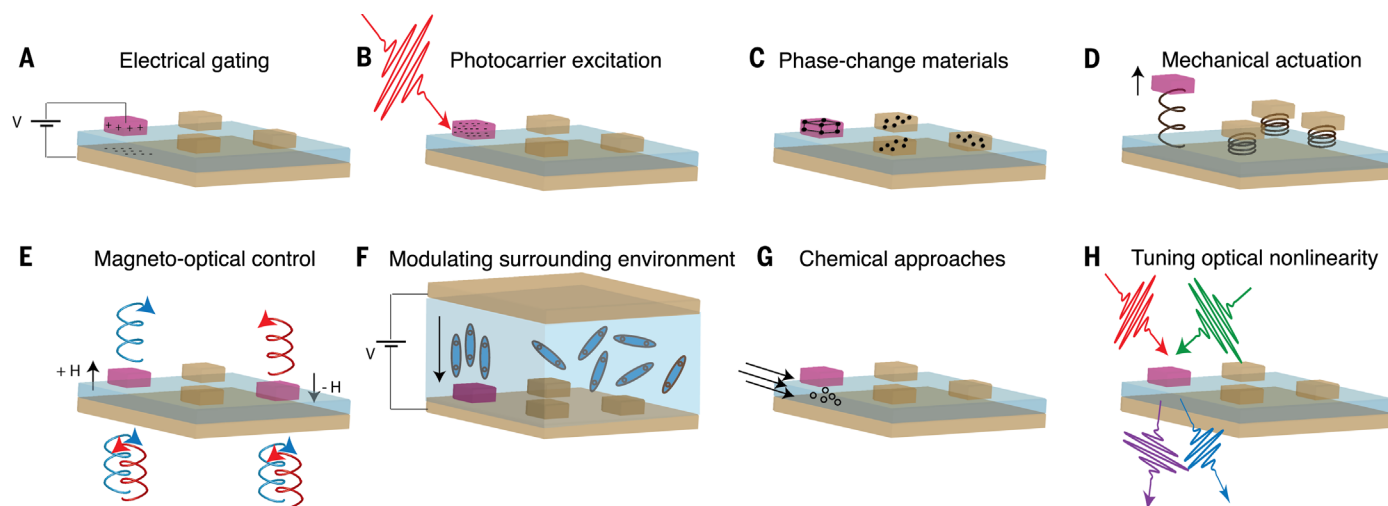


Fig. 1. Spatiotemporal processes in active metasurfaces. (A) Electrical gating can locally modify the free-carrier density and excitonic properties. (B) Photocarrier excitation induces changes in excited-carrier densities. (C) Phase-change materials experience modifications in their optical properties upon a structural or electronic phase transformation. (D) Mechanical actuation modifies optical response by controlling the spacing between nanostructures or their geometry. (E) Building blocks of magneto-optical materials exhibit distinct responses for circularly polar-

ized components upon stimulation by an external magnetic field H. (F) The dielectric environment of antennas can have a notable impact on their optical properties, and this affords effective tuning with, for example, liquid crystals. (G) Chemical reactions enable index changes through the creation of new molecules or the motion of ions through electrochemistry. (H) Optical nonlinearity enhanced by structural resonances can lead to ultrafast modulation of optical responses of a metasurface as well as frequency conversion.

modulation of an ultrathin GST layer integrated with a gold metasurface has been used to realize an all-optical metaswitch (Fig. 2D) (48). Metasurfaces can also be patterned directly into phase-change material itself to switch optical reflection and absorption properties or to generate anomalously reflected beams (58, 59). GST-based reconfigurable metasurfaces have also been achieved through beam shaping of optical pumps (60). Another approach has been used through coupling aluminum plasmonic antennas to GST material, and wavelength shifts have been demonstrated in the plasmonic resonances upon chang-

ing of the GST phase (61). Another prominent phase change material is VO₂ owing to its ability to undergo a metal-to-insulator transition upon changes in the temperature (Fig. 2E) (49). This material has been used to build thermally controlled ultrathin perfect absorbers (52) and to implement a thermally tunable terahertz lens (20). Layered VO₂-TiO₂ heterostructures have also provided valuable dispersion control, in which one can elicit a hyperbolic-to-elliptic phase transition (62). Nanoparticles of Ga have also featured a hysteric dependence in their optical response when the temperature is cir-

dled between 100 and 300 K (63). Later, a Ga-based metasurface has been demonstrated that uses a light-induced transition between solid and liquid phases of Ga by raising its temperature from 23.5° to 31.5° with low light intensity (microwatt per square micrometer) illumination, which experimentally achieved high-contrast all-optical switching in the near-IR range (55).

Mechanical actuation

Mechanical actuation offers a very effective way to tune metasurface properties by reconfiguring the shape and spatial arrangement of antennas

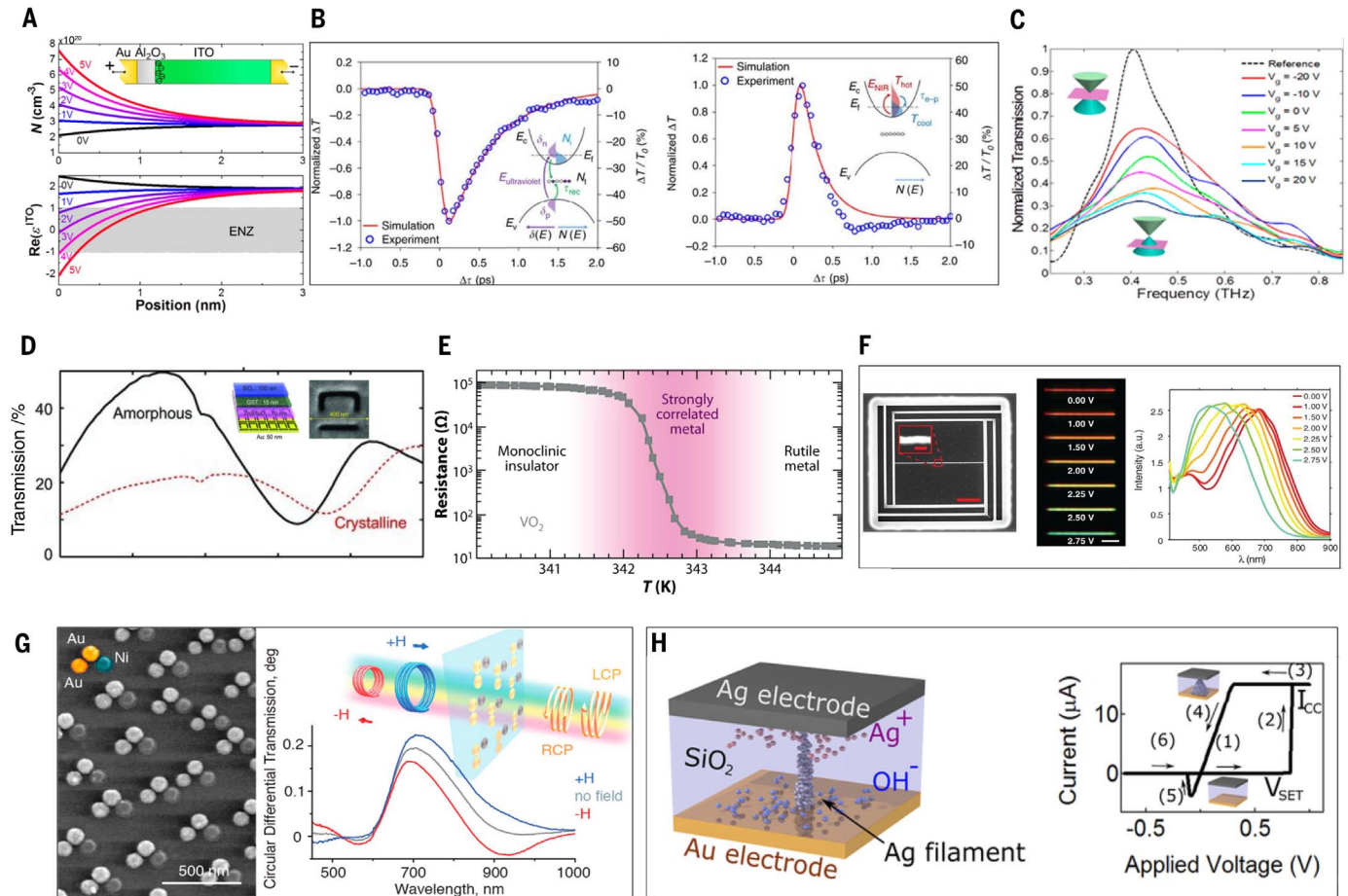


Fig. 2. Materials and building blocks of active metasurfaces.

(A) Operation of voltage-based gate-tunable metasurface. Applied voltage creates a nanoscale electron accumulation region in an ITO film. Shown are spatial distributions of carrier concentrations and associated real part of ITO permittivity with the ENZ region defined by permittivity between -1 and 1 (9). (B) Operation of optically excited AZO. (Left) Normalized change in transmission of a 1300-nm probe pulse applied to a 900-nm-thick AZO layer versus the pump-probe delay $\Delta\tau$ under 262 nm excitation. (Inset) The interband excitation process in which an ultraviolet pump generates electron-hole pairs (δn , δp) above the Fermi level (E_F). (Right) Normalized change in transmission of 1300 nm light versus the pump-probe delay $\Delta\tau$ under 787 nm excitation. (Inset) The process of intraband excitation. NIR light (E_{NIR}) raises the temperature of conduction band electrons ($T_{\text{cool}} \rightarrow T_{\text{hot}}$), which relax through scattering processes (τ_{e-p}) (30). (C) Transmission spectrum of a graphene-based metasurface for gate voltages in the range from -20 to $+20$ V. (Inset) Fermi-level shifts with gate

voltage that cause changes in optical properties (32). (D) Spectral response of optical transmission for both states of GST (amorphous versus crystalline) (48). (Inset) Structure of a GST-based metasurface and scanning electron microscopy (SEM) of a single unit cell. (E) Temperature-dependent metal-insulator-transition in VO₂ (49). (F) (Left) SEM of fabricated device with a silicon nanowire (NW) that is movable above a reflective silicon surface. (Middle) Dark-field images of the NW under transverse magnetic polarization and different applied voltages causing different elevations of the NW above a reflecting mirror and its color tuning. (Right) Dark-field scattering spectra confocally collected from the NW (65). (G) (Left) SEM of magneto-optical metasurface based in Au-Au-Ni trimer nanoantennas. (Right) Schematic of the magneto-optical metasurface and circular dichroism transmission data with (blue, red) and without (gray) applied magnetic field of about ± 3 kOe (73). (H) (Left) Electrochemical metallization-based unit cell (ECM), where Ag⁺ migration from anode to cathode creates a resistive switch. (Right) I - V curve of the ECM cell (80).

rather than altering their materials properties. Mature micro-electro-mechanical (MEMS) (19, 64, 65) technology also offers positioning and orientation control of nanostructures at subnanometer and subdegree angles. Mechanically controlled silicon nanoantennas have been implemented whose scattering spectral response is tunable across the entire visible spectrum by changing their elevation above a reflective surface (Fig. 2F) (65). Varifocal lenses have also been implemented by using one fixed and one movable metasurface lens (19). Its low mass offers higher operation speeds (kilohertz to megahertz) compared with those of conventional, bulky versions, and this opens the door to new ways for 3D imaging and reconfigurable optics. In another approach, mechanical configurability of metasurfaces has been achieved by constructing them from bilayered beams composed of gold and silicon nitride, which feature a high contrast in their thermal expansion coefficients (64). Temperature changes (76 to 270 K) then result in bending of the beams and an associated transmission modulation of 50% in the near-IR (64). Similar structures have also been used to enhance optical nonlinearities (66), in which a pump beam induces electromagnetic and thermal forces capable of reconfiguring structures to modulate probe beams. In another demonstration, Lorentz forces have been used to mechanically modulate nanostructures by use of strong magnetic fields (67).

Stretching of flexible substrates, such as polydimethylsiloxane (PDMS), is also well suited for tuning metasurface properties because the near-field and far-field interactions between antennas are very sensitive to their spacing (15, 17, 18, 21). A varifocal metasurface lens has been implemented by stretching by 30% the substrate it was placed on (15). Unidirectional stretching has also been used to achieve polarization-dependent tuning of dielectric metasurfaces (21). Even dynamic holograms have been created with a gold nanorod metasurface built on top of PDMS (15). Upon stretching the substrate, the location of the image plane changes and allows the structure to switch between three distinct images (15). Kirigami, the traditional Japanese art of cutting paper, has successfully been demonstrated at the nanoscale (68) and offers notable optical tuning by altering the overall shape of complex 3D structures (68, 69). Kirigami-based gratings have also been successfully applied to achieve laser beam steering by 6.5° of a diffracted beam (69). Last, structural tunability can also be achieved by building liquid metal-based nano-antennas.

Magneto-optic control

The impact of magnetic fields on optical materials properties tends to be relatively weak, and magnetic fields are hard to use for controlling metasurface behavior. However, magneto-optics can provide a fast, subnanosecond response (70) and can offer distinct opportunities to make polarization controllers or nonreciprocal devices (71). One can use this effect in the field of metasurfaces by either placing nanostructures on top of a magneto-optical substrate or by patterning the

magneto-optical material itself. In one implementation, gold gratings have been fabricated on top of a planar ferromagnetic dielectric grown over a nonmagnetic substrate (72). The structure exhibits magneto-plasmonic properties in which the plasmonic light concentration enhanced the magneto-optical Kerr effect. Similar structures have been used to modulate the intensity of a transmitted light beam by 24% through in-plane magnetic fields inside the ferromagnetic layer (70). Magneto-optical control has also been implemented toward the realization of chiro-optical metasurfaces. For example, a metasurface has been demonstrated whose unit cells are composed of three nanodisks each, two gold nanodisks to elicit a chiroptical behavior and one nickel nanodisk that provides the magneto-optical activity (Fig. 2G). Upon modulating an external magnetic field, the optical transmission is also modulated to produce a differential power transmission between left- and right-circularly polarized light (73).

Modulating the dielectric environment

The resonant properties of nanoantennas are highly sensitive to their dielectric environment because their modal fields extend somewhat beyond their physical boundaries. Therefore, tunable metasurfaces can also be realized by modulating the complex refractive index of the surroundings, such as with liquid crystals (74–78). This can be achieved by applying external electric fields capable of reorienting nematic liquid crystals (akin to Fig. 1F) (75). This strategy has been implemented with both Mie-resonant dielectric (75) and plasmonic (76, 78) metasurfaces to manipulate the amplitude and polarization state of light waves. Liquid crystals have also opened ways to thermally control metasurfaces (77) and facilitate active re-direction of laser beams (74).

Chemical approaches

Chemistry facilitates the creation of new materials and molecules that can have very distinct optical properties of the reactants. Electrochemical growth of nanometallic structures has enabled active spectral tuning of antennas (79–81). Because this type of chemistry involves movement of atoms, it is expected to be slow. However, in cleverly engineered systems only a few atoms need to move in and out of regions with high field concentration to achieve notable changes, and nanosecond-scale switching times can be realized. For example, electrically switchable antennas with active switching volumes below 5 nm³ have been realized. In those cases, the switching results from electrochemically displacing metal atoms to electrically connect two crossed metallic wires separated by a nanometer-scale gap (79). Demonstrated in Fig. 2H is another realization of electrochemical metallization through ion migration from anode to cathode, creating a resistive switch with a current-voltage (*I*-*V*) curve demonstrating switching between low and high resistances (80). Metasurfaces can also be dynamically controlled by running reactions on their surface. For example, a metallic metasurface has been

integrated with a layer of photoisomerizable molecules (16), which acts as a switching layer upon optical excitation with milliwatt-power levels. In a different work, electrical modulation of a metasurface response has been experimentally demonstrated by stimulating transport of silver ions in an alumina layer separating ITO and Ag electrodes (82). Images have even been created whose colors evolve upon hydrogenation of magnesium metasurfaces (83).

Tuning optical nonlinearity

Nonlinear processes afford valuable optical functions, such as ultrafast switching and signal processing, frequency conversion, and pulse generation. Metasurfaces can help to boost the typically weak photon-photon interactions in bulk materials by concentrating light in a nonlinear medium (84). Compared with uniform media, nanostructured nonlinear metasurfaces can also provide better control over the polarization, angle, and frequency-dependent nonlinear properties. For example, all-optical control of plasmonic nanoantennas embedded in ITO has been demonstrated, in which the optical nonlinearity of ITO is enhanced by means of plasmon-induced hot electron injection (38). In another implementation, gold antennas of varying lengths are positioned on top of an ITO layer (85). Upon excitation with spatially and spectrally distinct optical pumps, efficient transfer of a Kerr nonlinearity between the different elements is mediated by the ITO layer. This concept has also been used to enhance third harmonic generation produced by an ITO nanocrystal, which is placed in the hot spot of gold nanogap antennas (86). Entirely new electrically tunable nonlinear functions, such as frequency conversion, can also be achieved by incorporating nonlinear materials between patterned metallic metasurface electrodes that are electrically activated (87).

The metal (88) and semiconductor (89) antennas that make up metasurfaces can also provide strong nonlinearities themselves. Metals display sub-100-fs relaxation times for the carriers and thus offer ultrafast nonlinearities in metasurfaces (90). In this regard, a gold-based metasurface has been used in which the plasmonic confinement enhanced the optical nonlinearity of metals by several orders of magnitude (90). Highly anisotropic gold nanorods have also been used in a metasurface to modulate the state of light polarization at picosecond time scales (91). In a different manifestation of nonlinearities, semiconductor-based Mie resonators have been used to enhance and control nonlinear processes in metasurfaces (92). In this work, localized magnetic Mie resonances have been used to enhance two-photon absorption with respect to a nonstructured silicon film by a factor of 80. Mie resonances have also been used to enhance optical nonlinearities based on free-carrier injection (93), in which GaAs nanodisk resonances exhibit a 30-nm wavelength shift upon optical excitation. Last, metasurfaces add more degrees of freedom in controlling optical nonlinearities for nonlinear processes that require phase matching. For example, a phase-gradient

silicon metasurface has been used on top of a nonlinear lithium niobate layer and experimentally demonstrated a broadband phase matching-free second harmonic generation inside lithium niobate (94).

Several factors, such as the materials compatibility and operating speed, should be taken into consideration regarding the selection of the appropriate modulation technology. Certain new physical phenomena may only be accessible at very high modulation speeds. In such cases, suitable modulation techniques include ultrafast (10 fs to 0.5 ps) photo-carrier excitation (29) and optical nonlinearities in metals and semiconductors (90), or fast magneto-optical control with subnanosecond responses (70). Other relatively slower modulation techniques such as electrical gating (up to ~10 GHz) or mechanical actuation (kilohertz to megahertz) can also find many applications in reconfigurable devices. The choice of tuning mechanism is also dependent on possible ways to locally address single meta-atoms in large-area metasurfaces. For modulation schemes that rely on electrical actuation, the complexities associated with the electrical wiring and power consumption rival those of densely integrated circuits, where many active elements need to be switched simultaneously and at high speed. When the tunable optical functions are known, this challenge can be relaxed by electrically connecting antennas or modulating the surrounding environment of many antennas (such as the substrate). Optical switching of metasurfaces may become the only viable method of actuating metasurfaces at very high speeds.

Reconfigurable metasurfaces for active devices

The ability to manipulate free-space optical signals by using thin spatiotemporal metasurfaces is extremely appealing for many device applications. Such elements can enable effective and flexible mode conversion. This is important for optical communications, in which signals can be encoded into wavelength channels, optical spins, and linear or angular momenta. Dynamic wavefront control can also provide attractive solutions for many emerging technology applications in robotics, autonomous vehicles, augmented reality, analog optical computing, imaging, and holographic displays. In these, the replacement of bulky and power-consuming hardware with lighter, faster, and cost- and energy-efficient alternatives that can conveniently be integrated with electronics is critical. In the following section, key emerging applications of the spatiotemporal metasurface-based devices are presented. These include laser beam steering devices; varifocal lenses and dynamic holograms; and elements for dynamic amplitude, phase, and polarization control.

Beam steering and computational imaging

The applications of laser beam steering are diverse and include scanners, imaging systems, navigation, autonomous vehicles, and other computational imaging applications. Computational imaging systems involve an integration of the

sensing system and post-processing computation in order to obtain the required images. Post-processing enables higher-resolution retrieval of information beyond the hardware limitations of optical sensing, such as in the case of synthetic aperture radar (12). In this regard, spatiotemporal metasurfaces provide simplified acquisition systems with great flexibility by enabling the natural use of the spatial, angular, and spectral degrees of freedom of light. Spatiotemporal metasurfaces achieve nonmechanical beam steering similar to microwave radar phased arrays through writing a linear phase profile with a 2π reset (95); individual antennas should ideally reach local phase modulation over the full (0 to 2π) phase range.

Nevertheless, optical beam steering can still be obtained with partial phase modulation at the cost of a reduced power efficiency (8). In this regard, numerous efforts are being executed to leverage the phase response of tunable metasurfaces. Gate-tunable metasurfaces have experimentally enabled a phase shift of 180° and a ~30% change in reflectance by applying a 2.5-V gate bias (9). In their work, they used electrical free-carrier modulation to vary the complex refractive index of an ITO layer. The π phase shift is sufficient to dynamically switch back-reflected near-IR light between normal reflection and ± 1 order diffracted beams at frequencies exceeding 10 MHz (Fig. 3A) (9). An ITO-based gap-plasmonic metasurface has been demonstrated to modulate mid-IR light through judicious control of the resonant properties of the gap-plasmonic antennas from the under- to over-coupling regime, and reflection phase tunability over 180 degrees has been experimentally demonstrated (10). Graphene-loaded gold resonators have demonstrated gate-tunable phase modulation up to 237° for reflected light at an operating wavelength of $\lambda = 8.5 \mu\text{m}$ (8). This can afford phased-array beam steering efficiency of 23% for modulating the reflection angle up to 30° . Digitally controlled coding metasurfaces have also been used in which each unit cell in the metasurface loads a pin diode (11), and a microwave implementation that shows switching of radiation angles has been demonstrated. The methodology of digitally modulating metasurfaces can be extrapolated to the visible regime by relaxing the requirement on the phase modulation range. In another demonstration, the angle of anomalous refraction of light has been modulated from 11° to 15° through an interaction with a metasurface implemented on top of a stretchable substrate (18). As large-angle beam steering becomes available, it can facilitate LIDAR systems and new head-mounted display technologies, such as a virtual retinal display for which the eye's retina essentially becomes the screen (96).

Varifocal lenses and dynamic holograms

Varifocal lenses are highly valuable in optical imaging, biosensing, and optical characterization. Consequently, several demonstrations of tunable focusing lenses have been realized by the use of reconfigurable metasurfaces. A VO_2 -based metasurface has been implemented whose

optical intensity at the focal spot is thermally controlled (20). Tunable metasurface lenses in the red (Fig. 3B) (18) and IR (17) spectral ranges have been demonstrated by stretching the substrate, which modulated the gradient of the induced phase across the metasurface that controls the focal length. In a different implementation, varifocal lenses operating in the visible regime have been implemented by using metasurface doublets with a MEMS controllable antenna spacing (19). Dynamic holograms are more challenging because they require creation and tuning of complex antenna patterns. Universal spatiotemporal (3+1D) holograms require full phase control over the scattered light from individual antennas. Some techniques have been developed to obtain optical holograms with partial reconfigurability. A dynamic hologram with a gold nanorod metasurface placed on a stretchable substrate has been demonstrated (15). The hologram is designed to include three distinct images at three different confocal planes, and stretching the substrate changes the image plane to switch between those images (15). The technique of coding metasurfaces has been used to relax the condition of full phase modulation (13). In this demonstration, unit cells are only modulated by a 0 or π phase shift (corresponding to digital codes 0 or 1), and an optimization algorithm is used to determine the code of each unit cell to produce the required holographic images. Microwave implementation of this device has been demonstrated as a proof of concept by using diode-based unit cells (Fig. 3C) (13).

Dynamic amplitude, phase, and polarization control

Active spectral tuning of optical antenna resonances constitutes one of the most efficient and natural ways to achieve local amplitude and phase modulation of scattered light. One can also affect the state of polarization by tuning polarization-dependent resonances. For example, it has been shown how metasurface resonances for two different polarizations can be tuned simultaneously and in opposing directions by linearly stretching a dielectric metasurface (Fig. 3D) (21). Polarization conversion can also be achieved by using anisotropic optical antennas that are either tunable or integrated with a tunable medium (10, 16). Another implementation of polarization conversion used anisotropic strip antennas integrated with a tunable ITO layer (Fig. 3E) (10). Phase-modulation metasurfaces are mostly discussed for their application in laser beam steering and dynamic holograms. Other important applications include interferometry and spectroscopy. Graphene-based phase-tunable metasurfaces have been used in one arm of a Michelson-interferometer (Fig. 3F), which enabled detection of a moving object acting as the other arm's mirror with nanoscale precision (14).

New optical phenomena in ultrafast modulated metasurfaces

When we change the optical properties of dynamic metasurfaces at an ultrafast temporal

scale, some exotic new physical phenomena can become accessible. Light propagation through static metasurfaces has inherent fundamental physical limitations, such as Lorentz reciprocity and frequency conservation for light waves. Time-varying metasurfaces can overcome such limitations, empowering a new genus of optical devices. As the modulation rate of metasurfaces increases to approach the bandwidth of the optical signal,

nonreciprocal behavior becomes accessible. Light propagating through such metasurfaces also undergoes a Doppler-like wavelength shift. This effect relates to the time refraction effect, in which photons propagating through a medium with a time-varying refracting index undergo a shift in their frequency as time evolves (97). If temporal control is further accelerated until it's comparable with the optical cycle, then an even

higher control over the spatial and spectral properties of light can be achieved, including the ability to compress or spectrally manipulate pulses as well as the formation of wavenumber band gaps (98).

The ways in which light can interact with a medium whose optical properties are altered at an ultrafast time scale are illustrated in the dispersion diagram in Fig. 4A. When a wave

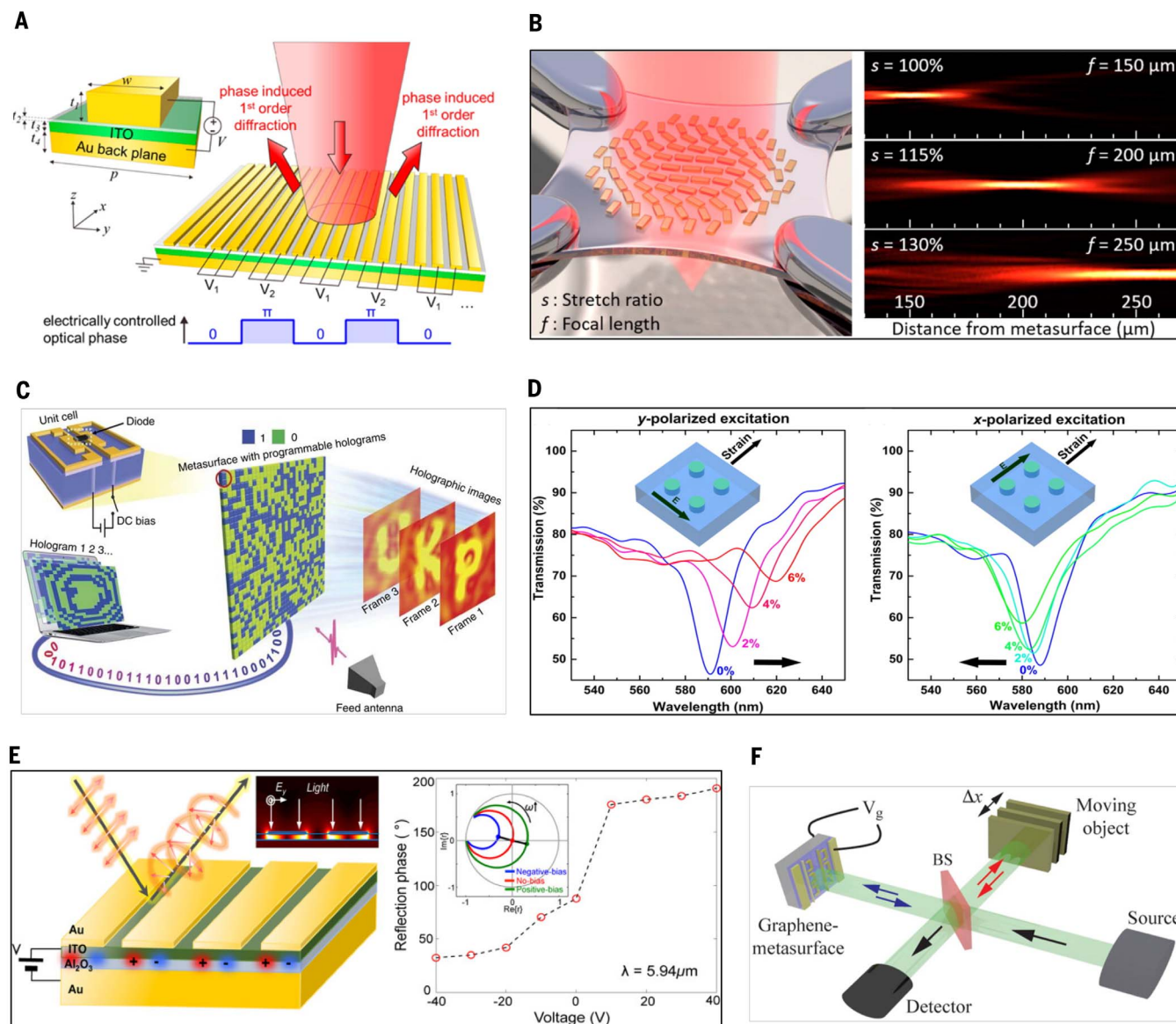


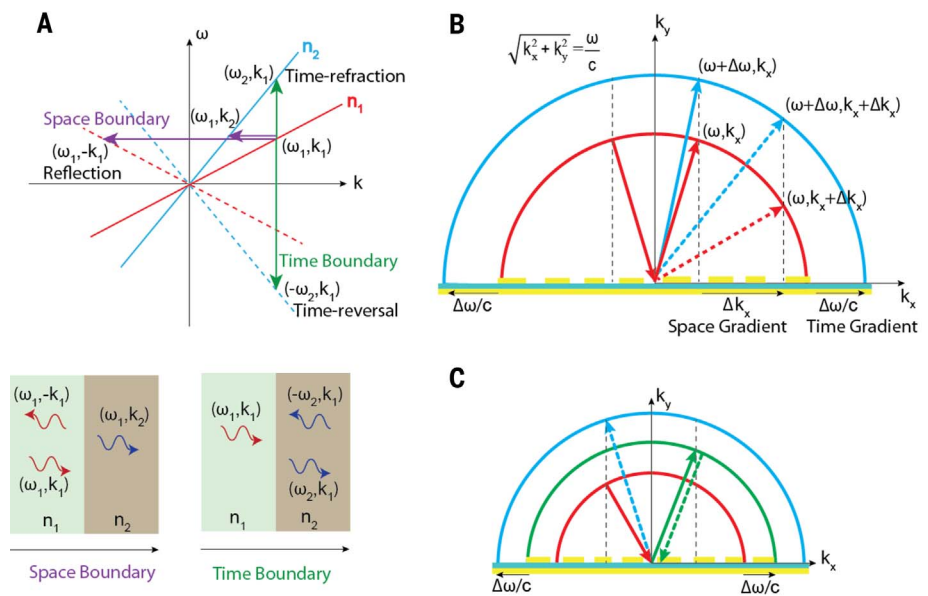
Fig. 3. Active devices using reconfigurable metasurfaces. (A) Gate-tunable metasurface-switching back-reflected light between normal reflection and ± 1 diffraction orders by inducing a π phase shift every other unit cell at a speed exceeding 10 MHz (9). (B) Tunable metalens capable of axial scanning throughout stretching its substrate. This creates a change into its phase gradient that in turn causes a variation of the focal length f as a function of the stretching ratios (18). (C) Reprogrammable coding metasurface. Different holographic images are produced as each of the metasurface elements is locally reprogrammed to induce phase shifts of 0 or π (corresponding to 0 or 1 digital codes). (Inset) Schematic of diode-based single unit cell (13). (D) Metasurface with a tunable resonant

wavelength, in which a stress applied to a stretchable substrate alters the separation between dielectric Mie resonant antennas along one of the two axes to induce a polarization-dependent resonant wavelength shift (21).

(E) (Left) Schematic of an electrically tunable metasurface design capable of tuning the phase of reflected light as well as modulating the polarization of incident light because of its anisotropic optical response. (Right) Phase modulation of reflected light from the electrically tunable metasurface versus applied electrical bias (10). (F) Schematic of interferometric motion detection by using graphene-based tunable metasurface, in which the motion of the reflecting object is detected by the phase of the reflected light from the tunable metasurface (14).

Fig. 4. Impact of spatiotemporal modulation on optical wave parameters (ω , k). (A) Dispers

sion relation illustrating the changes in frequency ω and linear momentum k as light crosses a spatial boundary (bottom left) or time boundary (bottom right) between media with different refractive indices n_1 and n_2 . Light with initial frequency/momentum values (ω_1, k_1) crossing a spatial boundary undergoes a change in momentum at a fixed frequency that generates a transmitted beam (ω_1, k_2) and a reflected beam $(\omega_1, -k_1)$. However, light crossing a time boundary (a homogeneous material switching from n_1 to n_2 in time) experiences a change in frequency that generates a forward time-refraction beam (ω_2, k_1) and a time-reversal beam $(-\omega_2, k_1)$. (B) Light interacting with spatiotemporal metasurfaces can change both its frequency ω and tangential momentum k_x . Reflection from a normal surface keeps the quantities (ω, k_x) unchanged, such as in the case of the solid red arrow, which represents Snell's law in which light is reflected at an angle identical to the angle of incidence. If the metasurface supports a reflection phase gradient, it will provide additional momentum to arrive at a point $(\omega, k_x + \Delta k_x)$, causing a redirection of the reflected beam (dashed red arrow) while keeping the light on the same isofrequency curve (red semicircle). Metasurfaces inducing time-varying phase shifts alternatively change the optical frequency and make the transition to a point $(\omega + \Delta\omega, k_x)$ on a new isofrequency circle (blue semicircle), leading to a new beam direction (solid blue arrow). A spatiotemporally modulated metasurface can in general create transitions in which both the frequency and momentum are independently modified to $(\omega + \Delta\omega, k_x + \Delta k_x)$, as indicated by the dashed blue arrow.



(C) Nonreciprocal time-varying metasurfaces. Incident light (red arrow) undergoes a wavelength shift upon reflection from a time-varying metasurface and reflects (green arrow) toward a new isofrequency curve (green semicircle), causing a deviation of Snell's law. A time-reversed beam (dashed green arrow) will also undergo a wavelength shift to generate a reflected beam (blue dashed arrow), pointing to a third isofrequency curve (blue semicircle) that is different from the isofrequency curve of the original incident beam (red semicircle). The nonreciprocal nature of the reflection from spatiotemporal metasurfaces is reflected in the difference between the incident red and blue arrows (24).

crosses a spatial boundary between two materials, its momentum changes while keeping its frequency constant. Similarly, light crossing a time boundary at which the refractive index of a homogeneous material is rapidly switched from n_1 to n_2 will experience complementary effects. In this case, the optical wave will display a frequency shift while keeping its momentum constant. This is a process known as time refraction (97, 99). Temporal boundary also induces another solution of Maxwell's equations that corresponds to the excitation of a negative frequency mode (100, 101). The $-\omega$ term corresponds to the signal under time reversal and leads to a backward-propagating, phase-conjugated (PC) wave (100).

In planar structures, time refraction can occur when a wave couples to a metasurface with a guided resonance. Frequency conversion can also be achieved by introducing a time-gradient phase discontinuity (24). In principle, both spatial and temporal phase shifts can be incurred from the same structure. For a general spatiotemporal phase shift $\psi(x, t)$, one can then alter both the frequency ω and tangential momentum k_x (Fig. 4B). Whereas spatial variations in a metasurface can impart changes in the tangential momentum $\Delta k_x = \partial\psi/\partial x$, time variations can modify the frequency $\Delta\omega = -\partial\psi/\partial t$ (24). This frequency shift is analogous to the conventional Doppler shift observed when light reflects from a

moving object, only in this case a stationary metasurface with time-varying optical properties is used. Furthermore, dynamic metasurfaces implemented at the surface of moving targets can modify the actual Doppler shift or even compensate for it, allowing for a Doppler Cloak that provides velocity invisibility (102).

Time-varying metasurfaces also have the ability to break Lorentz reciprocity and could meet all the requirements to build a magnetic-free optical isolator. It was shown that as a consequence of the Doppler-like frequency shift, a time-varying metasurface possesses a universal Snell's law that is not limited by Lorentz reciprocity (Fig. 4C) (24). This is attributed to the frequency shift "moving" the dispersion relation to a new isofrequency contour (Fig. 4, B and C). On the basis of this, time-varying metasurfaces should display a nonreciprocal Snell's law for incident and reflected or refracted waves upon excitation at oblique incidence (Fig. 4C). In the following section, we discuss proposed implementations and initial experimental realizations of the exotic phenomena displayed by spatiotemporal metasurfaces.

Frequency conversion and time refraction

The realization of the proposed exotic effects requires ultrafast modulation of induced phase shifts. It has been shown that atomically thin graphene microribbon arrays can potentially mod-

ulate the frequency of terahertz signals by gigahertz range values by using reflective metasurfaces in which the graphene is placed on top of a metallic layer separated by a dielectric spacer (103). Time refraction in an optically modulated AZO layer has been used to induce a notable 17-nm wavelength shift to a near-IR signal (104). In another implementation, linear frequency conversion of a terahertz signal has been realized by using a time-varying metasurface optically modulated by a near-IR pulse (27). In that work, arrays of double split-ring resonators were used to obtain two distinct resonances in the terahertz regime (Fig. 5A). The optical pump induces photo-carrier excitation in the optical gap between the two resonators, causing the resonant frequencies to merge into a single resonance. Upon changing the pulse delays, the resonant frequencies are seen to rapidly shift between the split and merged modes.

Time reversal and negative refraction

Time reversal and negative refraction (NR) are interrelated optical processes (100, 105), which are achievable by using time-dependent optical materials (101) or a four-wave mixing (FWM) optical nonlinear process (106). For example, backward PC and forward NR signals have been generated by using an ultrafast, optically modulated AZO thin layer (Fig. 5B). In a different manifestation, a FWM approach based on optical

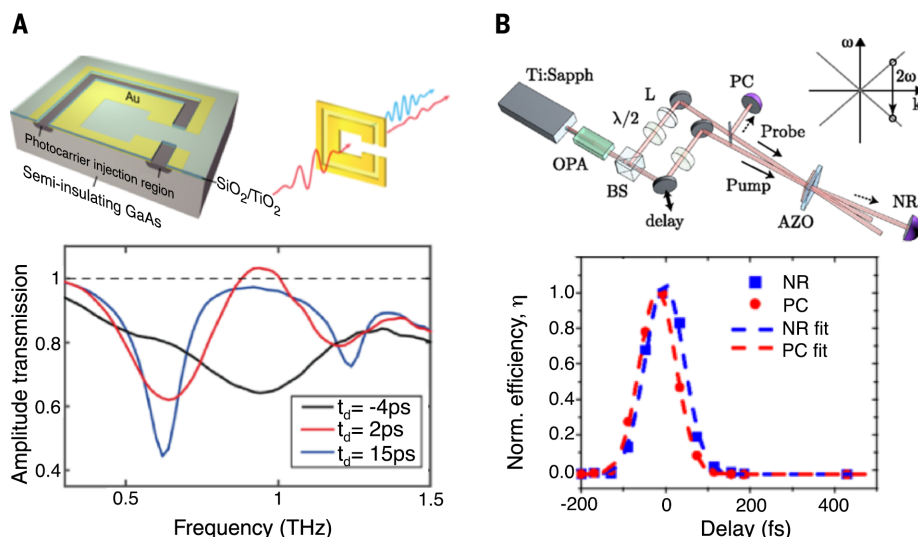


Fig. 5. Optical phenomena generated by ultrafast modulated metasurfaces. (A) (Top) Schematic of a unit cell of an optically tunable metasurface that affords frequency conversion. It consists of two split-ring resonators designed to resonate at 0.62 and 1.24 THz. They are separated by GaAs, which becomes conductive under NIR pump photocurrent generation, causing the combined structure to resonate at a new, single frequency of 0.92 THz. (Bottom) Spectral response of transmitted terahertz probe before NIR pump modulates the structure, showing two spectral resonances (blue curve). After the NIR pump excites the structure, it exhibits a single spectral resonance (black curve), and during the transient switching period (red curve), the two resonant frequencies shift with time between the blue and black curves (27). (B) (Top) Schematic of the experimental setup used to obtain a time-reversed or PC signal as well as a NR signal from a temporally modulated AZO layer. (Inset) A sketch of the time-reversal process as a transition from the point (k, ω) to the point $(k, -\omega)$ on the dispersion curve that corresponds to the generation of the PC and NR signals. (Bottom) The normalized intensity of the PC and NR signals as a function of pump-probe delay (101).

nonlinearities in an ultrathin graphite layer has been used to obtain PC and NR signals (106). It is worth noting that both PC and NR signals can restore optical features beyond the diffraction limit and therefore can be used in superresolution imaging applications (100, 101).

Nonreciprocity

Breaking optical reciprocity can lead to important photonic devices, such as flat optical isolators. Most optical isolators to date are based on the Faraday effect, which precludes densely integrated, on-chip implementations because of the requirements of large magnetic fields and long interaction lengths. Several alternative techniques have been proposed to realize nonreciprocity by using flat spatiotemporal metasurfaces. For example, realization of a nonreciprocal metasurface has been proposed by using an array of tunable photonic meta-atoms (26). Each individual meta-atom is composed of a dual-band resonator with two resonant frequencies. If the material of the resonator is temporally modulated at a frequency matching the difference between the two resonant frequencies, then the optical mode undergoes a transition from one resonant frequency to the other (26). This induced frequency shift causes a nonreciprocal change to the reflected/transmitted angle, as

predicted by a generalized Snell's law (akin to Fig. 4C) (24). An alternative route is suggested to achieve nonreciprocity while keeping the incident frequency unchanged (25). Hadad *et al.* designed a metasurface that displays a narrow-band transmission spectrum resulting from structural electromagnetic induced transparency (EIT). By temporally modulating this optical element, the transmission band for the forward-propagating waves is then shifted from the backward-propagating waves, dictating a unidirectional transmission at a specific wavelength (25). Kerr nonlinearities have also been used to achieve nonreciprocal metasurfaces. For example, a silicon-based metasurface has been designed in which a high-quality, factor-guided mode resonance structure was used to achieve a high tunability based on Kerr nonlinearity over only 100 nm thickness (107). On the basis of this tunability, a phase-gradient pattern to the structure creates an anomalous optical mode with nonreciprocal propagation (107).

These different manifestations of nonreciprocity show that for efficient isolation between forward- and backward-propagating waves, temporal modulation of the optical wave needs to be faster than its signal bandwidth. To reach such modulation speeds, one typically resorts to photocurrent excitation or ultrafast optical nonlinearities. However, the condition for fast modulation can be

relaxed if the optical signal is sufficiently narrow-band. For example, optical isolation for a near-IR optical signal has been realized by using gigahertz-speed optomechanical modulation, operating on a narrow-band optical signal inside a high-quality factor cavity (108).

Nonreciprocity paves the way toward achieving other interesting physical phenomena, such as creating topologically protected optical modes (28) and breaking reciprocity for thermal emission and absorption (109) in photovoltaic applications. Time-varying metasurfaces can also result in new studies that will explore modulation in the space-time domain, opening up new fields such as space-time transformation optics and spatiotemporal ultrafast coherent control of spatially localized molecular systems (110). As the switching speed of the material properties increases, new physical studies may arise that address how the fundamental processes of light absorption, emission, and modulation can be modified.

It is clear that the field of spatiotemporally modulated metasurfaces is highly underexplored and holds tremendous potential for new scientific discovery. We are just starting our journey to identify and learn about the materials, structures, and physics needed to create these new optical elements. At the same time, there is already a proven demand from industry to deliver lightweight, compact, and power-efficient flat optics capable of actively shaping the wavefront of light. Hopefully, this Review will bring further attention to this area and stimulate larger coordinated efforts.

REFERENCES AND NOTES

1. J. B. Pendry, D. Schurig, D. R. Smith, Controlling electromagnetic fields. *Science* **312**, 1780–1782 (2006). doi: [10.1126/science.1125907](https://doi.org/10.1126/science.1125907); pmid: [16728597](https://pubmed.ncbi.nlm.nih.gov/16728597/)
2. R. A. Shelby, D. R. Smith, S. Schultz, Experimental verification of a negative index of refraction. *Science* **292**, 77–79 (2001). doi: [10.1126/science.1058847](https://doi.org/10.1126/science.1058847); pmid: [11292865](https://pubmed.ncbi.nlm.nih.gov/11292865/)
3. Z. Bomzon, G. Biener, V. Kleiner, E. Hasman, Space-variant Pancharatnam-Berry phase optical elements with computer-generated subwavelength gratings. *Opt. Lett.* **27**, 1141–1143 (2002). doi: [10.1364/OL.27.001141](https://doi.org/10.1364/OL.27.001141); pmid: [18026387](https://pubmed.ncbi.nlm.nih.gov/18026387/)
4. N. Yu *et al.*, Light propagation with phase discontinuities: Generalized laws of reflection and refraction. *Science* **334**, 333–337 (2011). doi: [10.1126/science.1210713](https://doi.org/10.1126/science.1210713); pmid: [21885733](https://pubmed.ncbi.nlm.nih.gov/21885733/)
5. P. Lalanne, P. Chavel, Metalenses at visible wavelengths: Past, present, perspectives. *Laser Photonics Rev.* **11**, 1600295 (2017). doi: [10.1002/lpor.201600295](https://doi.org/10.1002/lpor.201600295)
6. Z. Lin, B. Grover, F. Capasso, A. W. Rodriguez, M. Lončar, Topology-optimized multilayered metaoptics. *Phys. Rev. Appl.* **9**, 044030 (2018). doi: [10.1103/PhysRevApplied.9.044030](https://doi.org/10.1103/PhysRevApplied.9.044030)
7. A. Nemat, Q. Wang, M. Hong, J. Teng, Tunable and reconfigurable metasurfaces and metadevices. *Opto-Electron. Rev.* **1**, 18000901–18000925 (2018).
8. M. C. Sherrott *et al.*, Experimental demonstration of >230° phase modulation in gate-tunable graphene-gold reconfigurable mid-infrared metasurfaces. *Nano Lett.* **17**, 3027–3034 (2017). doi: [10.1021/acs.nanolett.7b00359](https://doi.org/10.1021/acs.nanolett.7b00359); pmid: [28445068](https://pubmed.ncbi.nlm.nih.gov/28445068/)
9. Y. W. Huang *et al.*, Gate-tunable conducting oxide metasurfaces. *Nano Lett.* **16**, 5319–5325 (2016). doi: [10.1021/acs.nanolett.6b00555](https://doi.org/10.1021/acs.nanolett.6b00555); pmid: [27564012](https://pubmed.ncbi.nlm.nih.gov/27564012/)
10. J. Park, J. H. Kang, S. J. Kim, X. Liu, M. L. Brongersma, Dynamic reflection phase and polarization control in metasurfaces. *Nano Lett.* **17**, 407–413 (2017). doi: [10.1021/acs.nanolett.6b04378](https://doi.org/10.1021/acs.nanolett.6b04378); pmid: [27936784](https://pubmed.ncbi.nlm.nih.gov/27936784/)
11. X. Wan, M. Q. Qi, T. Y. Chen, T. J. Cui, Field-programmable beam reconfiguring based on digitally-controlled coding metasurface. *Sci. Rep.* **6**, 20663 (2016). doi: [10.1038/srep20663](https://doi.org/10.1038/srep20663); pmid: [26861110](https://pubmed.ncbi.nlm.nih.gov/26861110/)

12. A. Pedross-Engel, C. M. Watts, D. R. Smith, M. S. Reynolds, Enhanced resolution stripmap mode using dynamic metasurface antennas. *IEEE Trans. Geosci. Remote Sens.* **55**, 3764–3772 (2017). doi: [10.1109/TGRS.2017.2679438](https://doi.org/10.1109/TGRS.2017.2679438)
13. L. Li et al., Electromagnetic reprogrammable coding-metasurface holograms. *Nat. Commun.* **8**, 197 (2017). doi: [10.1038/s41467-017-00164-9](https://doi.org/10.1038/s41467-017-00164-9); pmid: 28775295
14. N. Dabidian et al., Experimental demonstration of phase modulation and motion sensing using graphene-integrated metasurfaces. *Nano Lett.* **16**, 3607–3615 (2016). doi: [10.1021/acs.nanolett.6b00732](https://doi.org/10.1021/acs.nanolett.6b00732); pmid: 27152557
15. S. C. Malek, H. S. Ee, R. Agarwal, Strain multiplexed metasurface holograms on a stretchable substrate. *Nano Lett.* **17**, 3641–3645 (2017). doi: [10.1021/acs.nanolett.7b00807](https://doi.org/10.1021/acs.nanolett.7b00807); pmid: 28488437
16. M.-X. Ren et al., Reconfigurable metasurfaces that enable light polarization control by light. *Light Sci. Appl.* **6**, e16254 (2017). doi: [10.1038/lsa.2016.254](https://doi.org/10.1038/lsa.2016.254); pmid: 30167257
17. S. M. Kamali, E. Arbabi, A. Arbabi, Y. Horie, A. Faraon, Highly tunable elastic dielectric metasurface lenses. *Laser Photonics Rev.* **10**, 1002–1008 (2016). doi: [10.1002/lpor.201600144](https://doi.org/10.1002/lpor.201600144)
18. H. S. Ee, R. Agarwal, Tunable metasurface and flat optical zoom lens on a stretchable substrate. *Nano Lett.* **16**, 2818–2823 (2016). doi: [10.1021/acs.nanolett.6b00618](https://doi.org/10.1021/acs.nanolett.6b00618); pmid: 26986191
19. E. Arbabi et al., MEMS-tunable dielectric metasurface lens. *Nat. Commun.* **9**, 812 (2018). doi: [10.1038/s41467-018-03155-6](https://doi.org/10.1038/s41467-018-03155-6); pmid: 29476147
20. J. He et al., Terahertz tunable metasurface lens based on vanadium dioxide phase transition. *Plasmonics* **11**, 1285–1290 (2016). doi: [10.1007/s11468-015-0173-2](https://doi.org/10.1007/s11468-015-0173-2)
21. P. Gutruf et al., Mechanically tunable dielectric resonator metasurfaces at visible frequencies. *ACS Nano* **10**, 133–141 (2016). doi: [10.1021/acsnano.5b05954](https://doi.org/10.1021/acsnano.5b05954); pmid: 26617198
22. J. Lee et al., Ultrafast electrically tunable polaritonic metasurfaces. *Adv. Opt. Mater.* **2**, 1057–1063 (2014). doi: [10.1002/adom.201400185](https://doi.org/10.1002/adom.201400185)
23. P. N. Dyachenko et al., Controlling thermal emission with refractory epsilon-near-zero metamaterials via topological transitions. *Nat. Commun.* **7**, 11809 (2016). doi: [10.1038/ncomms11809](https://doi.org/10.1038/ncomms11809); pmid: 27263653
24. A. Shaltout, A. Kildishev, V. Shalae, Time-varying metasurfaces and Lorentz non-reciprocity. *Opt. Mater. Express* **5**, 2459 (2015). doi: [10.1364/OME.5.002459](https://doi.org/10.1364/OME.5.002459)
25. Y. Hadad, D. L. Sounas, A. Alu, Space-time gradient metasurfaces. *Phys. Rev. B* **92**, 100304 (2015). doi: [10.1103/PhysRevB.92.100304](https://doi.org/10.1103/PhysRevB.92.100304)
26. Y. Shi, S. Fan, Dynamic non-reciprocal meta-surfaces with arbitrary phase reconfigurability based on photonic transition in meta-atoms. *Appl. Phys. Lett.* **108**, 021110 (2016). doi: [10.1063/1.4939915](https://doi.org/10.1063/1.4939915)
27. K. Lee et al., Linear frequency conversion via sudden merging of meta-atoms in time-variant metasurfaces. *Nat. Photonics* **12**, 765–773 (2018). doi: [10.1038/s41566-018-0259-4](https://doi.org/10.1038/s41566-018-0259-4)
28. K. Fang, Z. Yu, S. Fan, Realizing effective magnetic field for photons by controlling the phase of dynamic modulation. *Nat. Photonics* **6**, 782–787 (2012). doi: [10.1038/nphoton.2012.236](https://doi.org/10.1038/nphoton.2012.236)
29. M. Z. Alam, I. De Leon, R. W. Boyd, Large optical nonlinearity of indium tin oxide in its epsilon-near-zero region. *Science* **352**, 795–797 (2016). doi: [10.1126/science.aae0330](https://doi.org/10.1126/science.aae0330); pmid: 27127238
30. M. Clerici et al., Controlling hybrid nonlinearities in transparent conducting oxides via two-colour excitation. *Nat. Commun.* **8**, 15829 (2017). doi: [10.1038/ncomms15829](https://doi.org/10.1038/ncomms15829); pmid: 28598441
31. S. H. Lee et al., Switching terahertz waves with gate-controlled active graphene metamaterials. *Nat. Mater.* **11**, 936–941 (2012). doi: [10.1038/nmat3433](https://doi.org/10.1038/nmat3433); pmid: 23023552
32. W. Gao et al., High-contrast terahertz wave modulation by gated graphene enhanced by extraordinary transmission through ring apertures. *Nano Lett.* **14**, 1242–1248 (2014). doi: [10.1021/nl4041274](https://doi.org/10.1021/nl4041274); pmid: 24490772
33. M. Z. Alam, S. A. Schulz, J. Upham, I. De Leon, R. W. Boyd, Large optical nonlinearity of nanoantennas coupled to an epsilon-near-zero material. *Nat. Photonics* **12**, 79–83 (2018). doi: [10.1038/s41566-017-0089-9](https://doi.org/10.1038/s41566-017-0089-9)
34. L. Caspani et al., Enhanced nonlinear refractive index in e-near-zero materials. *Phys. Rev. Lett.* **116**, 233901 (2016). doi: [10.1103/PhysRevLett.116.233901](https://doi.org/10.1103/PhysRevLett.116.233901); pmid: 27341234
35. E. Feigenbaum, K. Diest, H. A. Atwater, Unity-order index change in transparent conducting oxides at visible frequencies. *Nano Lett.* **10**, 2111–2116 (2010). doi: [10.1021/nl1006307](https://doi.org/10.1021/nl1006307); pmid: 20481480
36. J. Park, J.-H. Kang, X. Liu, M. L. Brongersma, Electrically tunable epsilon-near-zero (ENZ) metamaterial absorbers. *Sci. Rep.* **5**, 15754 (2015). doi: [10.1038/srep15754](https://doi.org/10.1038/srep15754); pmid: 26549615
37. G. Kafaei Shirmanesh, R. Sokhoyan, R. A. Pala, H. A. Atwater, Dual-gated active metasurface at 1550 nm with wide (>300°) phase tunability. *Nano Lett.* **18**, 2957–2963 (2018). doi: [10.1021/acs.nanolett.8b00351](https://doi.org/10.1021/acs.nanolett.8b00351); pmid: 29570306
38. M. Abb, P. Albella, J. Aizpurua, O. L. Muskens, All-optical control of a single plasmonic nanoantenna-ITO hybrid. *Nano Lett.* **11**, 2457–2463 (2011). doi: [10.1021/nl200901w](https://doi.org/10.1021/nl200901w); pmid: 21542564
39. J. Gu et al., Active control of electromagnetically induced transparency analogue in terahertz metamaterials. *Nat. Commun.* **3**, 1151 (2012). doi: [10.1038/ncomms2153](https://doi.org/10.1038/ncomms2153); pmid: 23093188
40. Z. Fang et al., Active tunable absorption enhancement with graphene nanodisk arrays. *Nano Lett.* **14**, 299–304 (2014). doi: [10.1021/nl404042h](https://doi.org/10.1021/nl404042h); pmid: 24320874
41. V. W. Brar et al., Electronic modulation of infrared radiation in graphene plasmonic resonators. *Nat. Commun.* **6**, 7032 (2015). doi: [10.1038/ncomms8032](https://doi.org/10.1038/ncomms8032); pmid: 25948173
42. K. Wang et al., Electrical control of charged carriers and excitons in atomically thin materials. *Nat. Nanotechnol.* **13**, 128–132 (2018). doi: [10.1038/s41565-017-0030-x](https://doi.org/10.1038/s41565-017-0030-x); pmid: 29335564
43. Y. Yao et al., Broad electrical tuning of graphene-loaded plasmonic antennas. *Nano Lett.* **13**, 1257–1264 (2013). doi: [10.1021/nl3047943](https://doi.org/10.1021/nl3047943); pmid: 23441688
44. N. K. Emani et al., Electrically tunable damping of plasmonic resonances with graphene. *Nano Lett.* **12**, 5202–5206 (2012). doi: [10.1021/nl302322t](https://doi.org/10.1021/nl302322t); pmid: 22950873
45. Y. Yao et al., Electrically tunable metasurface perfect absorbers for ultrathin mid-infrared optical modulators. *Nano Lett.* **14**, 6526–6532 (2014). doi: [10.1021/nl503104n](https://doi.org/10.1021/nl503104n); pmid: 25310847
46. K. Wang et al., Ultrafast nonlinear excitation dynamics of black phosphorus nanosheets from visible to mid-infrared. *ACS Nano* **10**, 6923–6932 (2016). doi: [10.1021/acsnano.6b02770](https://doi.org/10.1021/acsnano.6b02770); pmid: 27281449
47. E. M. Mannebach et al., Dynamic optical tuning of interlayer interactions in the transition metal dichalcogenides. *Nano Lett.* **17**, 7761–7766 (2017). doi: [10.1021/acs.nanolett.7b03955](https://doi.org/10.1021/acs.nanolett.7b03955); pmid: 29119791
48. B. Gholipour, J. Zhang, K. F. MacDonald, D. W. Hewak, N. I. Zheludev, An all-optical, non-volatile, bidirectional, phase-change meta-switch. *Adv. Mater.* **25**, 3050–3054 (2013). doi: [10.1002/adma.201300588](https://doi.org/10.1002/adma.201300588); pmid: 23625824
49. Z. Yang, C. Ko, S. Ramanathan, Oxide electronics utilizing ultrafast metal-insulator transitions. *Annu. Rev. Mater. Res.* **41**, 337–367 (2011). doi: [10.1146/annurev-matsci-062910-100347](https://doi.org/10.1146/annurev-matsci-062910-100347)
50. J. Rensberg et al., Active optical metasurfaces based on defect-engineered phase-transition materials. *Nano Lett.* **16**, 1050–1055 (2016). doi: [10.1021/acs.nanolett.5b04122](https://doi.org/10.1021/acs.nanolett.5b04122); pmid: 26690855
51. H. N. S. Krishnamoorthy, Y. Zhou, S. Ramanathan, E. Narimanov, V. M. Menon, Tunable hyperbolic metamaterials utilizing phase change heterostructures. *Appl. Phys. Lett.* **104**, 121101 (2014). doi: [10.1063/1.4869297](https://doi.org/10.1063/1.4869297)
52. M. A. Kats et al., Ultra-thin perfect absorber employing a tunable phase change material. *Appl. Phys. Lett.* **101**, 221101 (2012). doi: [10.1063/1.4767646](https://doi.org/10.1063/1.4767646)
53. K. Dong et al., A lithography-free and field-programmable photonic metacanvas. *Adv. Mater.* **30**, 1703878 (2018). doi: [10.1002/adma.201703878](https://doi.org/10.1002/adma.201703878); pmid: 29226459
54. Z. Zhu, P. G. Evans, R. F. Haglund Jr., J. G. Valentine, Dynamically reconfigurable metadvice employing nanostructured phase-change materials. *Nano Lett.* **17**, 4881–4885 (2017). doi: [10.1021/acs.nanolett.7b01767](https://doi.org/10.1021/acs.nanolett.7b01767); pmid: 28731722
55. R. F. Waters, P. A. Hobson, K. F. MacDonald, N. I. Zheludev, Optically switchable photonic metasurfaces. *Appl. Phys. Lett.* **107**, 081102 (2015). doi: [10.1063/1.4929396](https://doi.org/10.1063/1.4929396)
56. M. Wuttig, N. Yamada, Phase-change materials for rewritable data storage. *Nat. Mater.* **6**, 824–832 (2007). doi: [10.1038/nmat2009](https://doi.org/10.1038/nmat2009); pmid: 17972937
57. K. Shportko et al., Resonant bonding in crystalline phase-change materials. *Nat. Mater.* **7**, 653–658 (2008). doi: [10.1038/nmat2226](https://doi.org/10.1038/nmat2226); pmid: 18622406
58. A. Karvounis, B. Gholipour, K. F. MacDonald, N. I. Zheludev, All-dielectric phase-change reconfigurable metasurface. *Appl. Phys. Lett.* **109**, 051103 (2016). doi: [10.1063/1.4959272](https://doi.org/10.1063/1.4959272)
59. C. R. de Galarreta et al., Nonvolatile reconfigurable phase-change metadvice for beam steering in the near infrared. *Adv. Funct. Mater.* **28**, 1704993 (2018). doi: [10.1002/adfm.201704993](https://doi.org/10.1002/adfm.201704993)
60. Q. Wang et al., Optically reconfigurable metasurfaces and photonic devices based on phase change materials. *Nat. Photonics* **10**, 60–65 (2015). doi: [10.1038/nphoton.2015.247](https://doi.org/10.1038/nphoton.2015.247)
61. A.-K. U. Michel et al., Using low-loss phase-change materials for mid-infrared antenna resonance tuning. *Nano Lett.* **13**, 3470–3475 (2013). doi: [10.1021/nl4006194](https://doi.org/10.1021/nl4006194); pmid: 23742151
62. H. N. S. Krishnamoorthy, Z. Jacob, E. Narimanov, I. Kretzschmar, V. M. Menon, Topological transitions in metamaterials. *Science* **336**, 205–209 (2012). doi: [10.1126/science.1219171](https://doi.org/10.1126/science.1219171); pmid: 22499943
63. K. F. MacDonald, V. A. Fedotov, N. I. Zheludev, Optical nonlinearity resulting from a light-induced structural transition in gallium nanoparticles. *Appl. Phys. Lett.* **82**, 1087–1089 (2003). doi: [10.1063/1.1543644](https://doi.org/10.1063/1.1543644)
64. J. Y. Ou, E. Plum, L. Jiang, N. I. Zheludev, Reconfigurable photonic metamaterials. *Nano Lett.* **11**, 2142–2144 (2011). doi: [10.1021/nl200791r](https://doi.org/10.1021/nl200791r); pmid: 21480583
65. A. L. Holsteen, S. Raza, P. Fan, P. G. Kik, M. L. Brongersma, Purcell effect for active tuning of light scattering from semiconductor optical antennas. *Science* **358**, 1407–1410 (2017). doi: [10.1126/science.aao5371](https://doi.org/10.1126/science.aao5371); pmid: 29242341
66. J. Y. Ou, E. Plum, J. Zhang, N. I. Zheludev, Giant nonlinearity of an optically reconfigurable plasmonic metamaterial. *Adv. Mater.* **28**, 729–733 (2016). doi: [10.1002/adma.201504467](https://doi.org/10.1002/adma.201504467); pmid: 26619205
67. J. Valente, J.-Y. Ou, E. Plum, I. J. Youngs, N. I. Zheludev, A magneto-electro-optical effect in a plasmonic nanowire material. *Nat. Commun.* **6**, 7021 (2015). doi: [10.1038/ncomms8021](https://doi.org/10.1038/ncomms8021); pmid: 25906761
68. T. C. Shyu et al., A kirigami approach to engineering elasticity in nanocomposites through patterned defects. *Nat. Mater.* **14**, 785–789 (2015). doi: [10.1038/nmat4327](https://doi.org/10.1038/nmat4327); pmid: 26099109
69. L. Xu et al., Kirigami nanocomposites as wide-angle diffraction gratings. *ACS Nano* **10**, 6156–6162 (2016). doi: [10.1021/acsnano.6b02096](https://doi.org/10.1021/acsnano.6b02096); pmid: 27152860
70. V. I. Belotelov et al., Plasmon-mediated magneto-optical transparency. *Nat. Commun.* **4**, 2128 (2013). doi: [10.1038/ncomms3128](https://doi.org/10.1038/ncomms3128); pmid: 23839481
71. A. Christofi, Y. Kawaguchi, A. Alù, A. B. Khanikaev, Giant enhancement of Faraday rotation due to electromagnetically induced transparency in all-dielectric magneto-optical metasurfaces. *Opt. Lett.* **43**, 1838–1841 (2018). doi: [10.1364/OL.43.001838](https://doi.org/10.1364/OL.43.001838); pmid: 29652378
72. V. I. Belotelov et al., Enhanced magneto-optical effects in magnetoplasmonic crystals. *Nat. Nanotechnol.* **6**, 370–376 (2011). doi: [10.1038/nnano.2011.54](https://doi.org/10.1038/nnano.2011.54); pmid: 21516090
73. I. Zubritskaya, N. Maccaferri, X. Inchausti Ezeiza, P. Vavassori, A. Dmitriev, Magnetic control of the chiroptical plasmonic surfaces. *Nano Lett.* **18**, 302–307 (2018). doi: [10.1021/acs.nanolett.7b04139](https://doi.org/10.1021/acs.nanolett.7b04139); pmid: 29240446
74. A. Komar et al., Dynamic beam switching by liquid crystal tunable dielectric metasurfaces. *ACS Photonics* **5**, 1742–1748 (2018). doi: [10.1021/acsp Photonics.7b01343](https://doi.org/10.1021/acsp Photonics.7b01343)
75. A. Komar et al., Electrically tunable all-dielectric optical metasurfaces based on liquid crystals. *Appl. Phys. Lett.* **110**, 071109 (2017). doi: [10.1063/1.4976504](https://doi.org/10.1063/1.4976504)
76. M. Decker et al., Electro-optical switching by liquid-crystal controlled metasurfaces. *Opt. Express* **21**, 8879–8885 (2013). doi: [10.1364/OE.21.008879](https://doi.org/10.1364/OE.21.008879); pmid: 23571978
77. J. Sautter et al., Active tuning of all-dielectric metasurfaces. *ACS Nano* **9**, 4308–4315 (2015). doi: [10.1021/acsnano.5b00723](https://doi.org/10.1021/acsnano.5b00723); pmid: 25748581
78. Y. U. Lee et al., Electro-optic switching in phase-discontinuity complementary metasurface twisted nematic cell. *Opt. Express* **22**, 20816–20827 (2014). doi: [10.1364/OE.22.020816](https://doi.org/10.1364/OE.22.020816); pmid: 25321285
79. D. T. Schoen, A. L. Holsteen, M. L. Brongersma, Probing the electrical switching of a memristive optical antenna by STEM EELS. *Nat. Commun.* **7**, 12162 (2016). doi: [10.1038/ncomms21262](https://doi.org/10.1038/ncomms21262); pmid: 27412052
80. G. Di Martino, S. Tappertzhofen, S. Hofmann, J. Baumberg, Nanoscale plasmon-enhanced spectroscopy in memristive switches. *Small* **12**, 1334–1341 (2016). doi: [10.1002/sml.201503165](https://doi.org/10.1002/sml.201503165); pmid: 26756792
81. U. Koch, C. Hoessbacher, A. Emboras, J. Leuthold, Optical memristive switches. *J. Electroceram.* **39**, 239–250 (2017). doi: [10.1007/s10832-017-0072-3](https://doi.org/10.1007/s10832-017-0072-3)
82. K. Thyagarajan, R. Sokhoyan, L. Zornberg, H. A. Atwater, Millivolt modulation of plasmonic metasurface optical

- response via ionic conductance. *Adv. Mater.* **29**, 1701044 (2017). doi: [10.1002/adma.201701044](https://doi.org/10.1002/adma.201701044); pmid: [28612946](https://pubmed.ncbi.nlm.nih.gov/28612946/)
83. X. Duan, S. Kamin, N. Liu, Dynamic plasmonic colour display. *Nat. Commun.* **8**, 14606 (2017). doi: [10.1038/ncomms14606](https://doi.org/10.1038/ncomms14606); pmid: [28232722](https://pubmed.ncbi.nlm.nih.gov/28232722/)
 84. B. Metzger, M. Hentschel, H. Giessen, Ultrafast nonlinear plasmonic spectroscopy: From dipole nanoantennas to complex hybrid plasmonic structures. *ACS Photonics* **3**, 1336–1350 (2016). doi: [10.1021/acsp Photonics.5b00587](https://doi.org/10.1021/acsp Photonics.5b00587)
 85. M. Abb, Y. Wang, C. H. de Groot, O. L. Muskens, Hotspot-mediated ultrafast nonlinear control of multifrequency plasmonic nanoantennas. *Nat. Commun.* **5**, 4869 (2014). doi: [10.1038/ncomms5869](https://doi.org/10.1038/ncomms5869); pmid: [25189713](https://pubmed.ncbi.nlm.nih.gov/25189713/)
 86. B. Metzger et al., Doubling the efficiency of third harmonic generation by positioning ITO nanocrystals into the hot-spot of plasmonic gap-antennas. *Nano Lett.* **14**, 2867–2872 (2014). doi: [10.1021/nl500913t](https://doi.org/10.1021/nl500913t); pmid: [24730433](https://pubmed.ncbi.nlm.nih.gov/24730433/)
 87. L. Kang et al., Electrifying photonic metamaterials for tunable nonlinear optics. *Nat. Commun.* **5**, 4680 (2014). doi: [10.1038/ncomms5680](https://doi.org/10.1038/ncomms5680); pmid: [25109813](https://pubmed.ncbi.nlm.nih.gov/25109813/)
 88. M. Kauranen, A. V. Zayats, Nonlinear plasmonics. *Nat. Photonics* **6**, 737–748 (2012). doi: [10.1038/nphoton.2012.244](https://doi.org/10.1038/nphoton.2012.244)
 89. Y. Kivshar, All-dielectric meta-optics and non-linear nanophotonics. *Natl. Sci. Rev.* **5**, 144–158 (2018). doi: [10.1093/nsr/nwy017](https://doi.org/10.1093/nsr/nwy017)
 90. M. Ren et al., Nanostructured plasmonic medium for terahertz bandwidth all-optical switching. *Adv. Mater.* **23**, 5540–5544 (2011). doi: [10.1002/adma.201103162](https://doi.org/10.1002/adma.201103162); pmid: [22021040](https://pubmed.ncbi.nlm.nih.gov/22021040/)
 91. L. H. Nicholls et al., Ultrafast synthesis and switching of light polarization in nonlinear anisotropic metamaterials. *Nat. Photonics* **11**, 628–633 (2017). doi: [10.1038/s41566-017-0002-6](https://doi.org/10.1038/s41566-017-0002-6)
 92. M. R. Shcherbakov et al., Ultrafast all-optical switching with magnetic resonances in nonlinear dielectric nanostructures. *Nano Lett.* **15**, 6985–6990 (2015). doi: [10.1021/acs.nanolett.5b02989](https://doi.org/10.1021/acs.nanolett.5b02989); pmid: [26393983](https://pubmed.ncbi.nlm.nih.gov/26393983/)
 93. M. R. Shcherbakov et al., Ultrafast all-optical tuning of direct-gap semiconductor metasurfaces. *Nat. Commun.* **8**, 17 (2017). doi: [10.1038/s41467-017-00019-3](https://doi.org/10.1038/s41467-017-00019-3); pmid: [28500308](https://pubmed.ncbi.nlm.nih.gov/28500308/)
 94. C. Wang et al., Metasurface-assisted phase-matching-free second harmonic generation in lithium niobate waveguides. *Nat. Commun.* **8**, 2098 (2017). doi: [10.1038/s41467-017-02189-6](https://doi.org/10.1038/s41467-017-02189-6); pmid: [29235473](https://pubmed.ncbi.nlm.nih.gov/29235473/)
 95. P. F. McManamon et al., A review of phased array steering for narrow-band electrooptical systems. *Proc. IEEE* **97**, 1078–1096 (2009). doi: [10.1109/JPROC.2009.2017218](https://doi.org/10.1109/JPROC.2009.2017218)
 96. E. Viirre, H. Pryor, S. Nagata, T. A. Furness 3rd, The virtual retinal display: A new technology for virtual reality and augmented vision in medicine. *Stud. Health Technol. Inform.* **50**, 252–257 (1998). pmid: [10180549](https://pubmed.ncbi.nlm.nih.gov/10180549/)
 97. L. O. E. Silva, J. T. Mendonça, G. N. Figueira, Theory of photon acceleration. *Phys. Scr. T* **63**, 222 (2001).
 98. F. Biancalana, A. Amann, A. V. Uskov, E. P. O'Reilly, Dynamics of light propagation in spatiotemporal dielectric structures. *Phys. Rev. E Stat. Nonlin. Soft Matter Phys.* **75**, 046607 (2007). doi: [10.1103/PhysRevE.75.046607](https://doi.org/10.1103/PhysRevE.75.046607); pmid: [17501007](https://pubmed.ncbi.nlm.nih.gov/17501007/)
 99. Y. Xiao, D. N. Maywar, G. P. Agrawal, Reflection and transmission of electromagnetic waves at a temporal boundary. *Opt. Lett.* **39**, 574–577 (2014). doi: [10.1364/OL.39.000574](https://doi.org/10.1364/OL.39.000574); pmid: [24487869](https://pubmed.ncbi.nlm.nih.gov/24487869/)
 100. J. B. Pendry, Time reversal and negative refraction. *Science* **322**, 71–73 (2008). doi: [10.1126/science.1162087](https://doi.org/10.1126/science.1162087); pmid: [18755940](https://pubmed.ncbi.nlm.nih.gov/18755940/)
 101. S. Vezzoli et al., Optical time reversal from time-dependent epsilon-near-zero media. *Phys. Rev. Lett.* **120**, 043902 (2018). doi: [10.1103/PhysRevLett.120.043902](https://doi.org/10.1103/PhysRevLett.120.043902); pmid: [29437435](https://pubmed.ncbi.nlm.nih.gov/29437435/)
 102. D. Ramaccia, D. L. Sounas, A. Alù, A. Toscano, F. Bilotti, Doppler cloak restores invisibility to objects in relativistic motion. *Phys. Rev. B* **95**, 075113 (2017). doi: [10.1103/PhysRevB.95.075113](https://doi.org/10.1103/PhysRevB.95.075113)
 103. Z. Liu, Z. Li, K. Aydin, Time-varying metasurfaces based on graphene microribbon arrays. *ACS Photonics* **3**, 2035–2039 (2016). doi: [10.1021/acsp Photonics.6b00653](https://doi.org/10.1021/acsp Photonics.6b00653)
 104. A. Shaltout et al., Doppler shift emulation using highly time-refractive TCO layer. *Conference on Lasers and Electro-Optics* (2016).
 105. V. Baco, M. Labousse, A. Eddi, M. Fink, E. Fort, Time reversal and holography with spacetime transformations. *Nat. Phys.* **12**, 972–977 (2016). doi: [10.1038/nphys3810](https://doi.org/10.1038/nphys3810)
 106. H. Harutyunyan, R. Beams, L. Novotny, Controllable optical negative refraction and phase conjugation in graphite thin films. *Nat. Phys.* **9**, 423–425 (2013). doi: [10.1038/nphys2618](https://doi.org/10.1038/nphys2618)
 107. M. Lawrence, D. R. Barton 3rd, J. A. Dionne, Nonreciprocal flat optics with silicon metasurfaces. *Nano Lett.* **18**, 1104–1109 (2018). doi: [10.1021/acs.nanolett.7b04646](https://doi.org/10.1021/acs.nanolett.7b04646); pmid: [29369641](https://pubmed.ncbi.nlm.nih.gov/29369641/)
 108. K. Fang et al., Generalized non-reciprocity in an optomechanical circuit via synthetic magnetism and reservoir engineering. *Nat. Phys.* **13**, 465–471 (2017). doi: [10.1038/nphys4009](https://doi.org/10.1038/nphys4009)
 109. Y. Hadad, J. C. Soric, A. Alu, Breaking temporal symmetries for emission and absorption. *Proc. Natl. Acad. Sci. U.S.A.* **113**, 3471–3475 (2016). doi: [10.1073/pnas.1517363113](https://doi.org/10.1073/pnas.1517363113); pmid: [26984502](https://pubmed.ncbi.nlm.nih.gov/26984502/)
 110. L. Piatkowski, N. Accanto, N. F. van Hulst, Ultrafast meets ultrasmall: Controlling nanoantennas and molecules. *ACS Photonics* **3**, 1401–1414 (2016). doi: [10.1021/acsp Photonics.6b00124](https://doi.org/10.1021/acsp Photonics.6b00124)

ACKNOWLEDGMENTS

Funding: This work was supported by the Air Force Office of Scientific Research (AFOSR) under Multidisciplinary University Research Initiative grant FA9550-14-1-0389. M.L.B. also acknowledges support from an individual investigator grants FA9550-17-1-0331 and FA9550-18-1-0323 from the AFOSR and the U.S. Department of Energy (DOE) "Photonics at Thermodynamic Limits" Energy Frontier Research Center under grant DE-SC0019140. V.M.S. also acknowledges support by the DOE Office of Basic Energy Sciences, Division of Materials Sciences and Engineering under award DE-SC0017717 (ENZ active metasurfaces) and AFOSR grant FA9550-18-1-0002 (space-time metasurfaces). **Competing interests:** None declared.

10.1126/science.aat3100

Spatiotemporal light control with active metasurfaces

Amr M. Shaltout, Vladimir M. Shalaev and Mark L. Brongersma

Science **364** (6441), eaat3100.
DOI: 10.1126/science.aat3100

Dynamic metasurfaces

Optical metasurfaces have opened an entirely new field in the quest to manipulate light. Optical metasurfaces can locally impart changes to the amplitude, phase, and polarization of propagating waves. To date, most of these metasurfaces have been passive, with the optical properties largely set in the fabrication process. Shaltout *et al.* review recent developments toward time-varying metasurfaces and explore the opportunities that adding dynamic control can offer in terms of actively controlling the flow of light.

Science, this issue p. eaat3100

ARTICLE TOOLS

<http://science.sciencemag.org/content/364/6441/eaat3100>

REFERENCES

This article cites 109 articles, 8 of which you can access for free
<http://science.sciencemag.org/content/364/6441/eaat3100#BIBL>

PERMISSIONS

<http://www.sciencemag.org/help/reprints-and-permissions>

Use of this article is subject to the [Terms of Service](#)